

Dramatic Anisotropy of Organic Superconducting Thin Film Formation on (TMTSF)₂PF₆ Single-Crystal Templates

Angelina Angelova, Alec Moradpour,* Pascale Auban-Senzier, Nor-Eddine Akaaboune, and Claude Pasquier

Laboratoire de Physique des Solides, UMR C8502 of CNRS, University Paris-Sud, F-91405 Orsay Cedex, France

Received February 28, 2000. Revised Manuscript Received May 19, 2000

The generation of (TMTSF)₂ClO₄ overlayers on (TMTSF)₂PF₆ single crystals, obtained by immersing templates in 1,1,2-trichloroethane at room temperature, is shown to be highly anisotropic. Well-defined 5–15 μm thick films are formed exclusively on the (011) faces of the crystal. These films are found to be superconducting by conductivity measurements. The electrochemical formation of (TMTSF)₂ClO₄ overlayers, under the same solution conditions, only takes place by epitaxial overgrowth onto the (001) faces.

Introduction

The conditions required for obtaining organic superconducting thin films involve (i) the creation of highly ordered single-crystal thin films and (ii) the thermal expansion coefficient of the film to be comparable to that of the underlying substrate, in addition to commensurable crystal lattice parameters. This set of requirements is hardly fulfilled by the methods generally used for the preparation of organic thin films,¹ e.g. self-assembly techniques based on molecular recognition and surface chemical reactions, multilayer deposition by the Langmuir–Blodgett method, spin-coatings, molecular beam epitaxy, or chemical and photochemical vapor-phase deposition methods. Nonetheless, attempts toward the preparation of organic superconducting films by evaporation techniques have been reported^{2–4} but they resulted in poorly ordered polycrystalline solids (condition (i) not achieved). On the other hand, electrochemically mediated epitaxy of (bulk superconducting) BEDT-TTF salts (BEDT-TTF: bis(ethylenedithio)tetrathiafulvalene) on graphite⁵ yielded well-defined crystal overgrowth, although condition ii, needed to adequately characterize superconductivity, is not satisfied in this interesting study. The reliable generation of superconducting single-crystal organic thin films requires therefore specific new methodologies. The formation of such thin films has only been reported very recently.^{6,7}

In a previous study we have reported that overlayers of the quasi-1D superconductor (TMTSF)₂ClO₄ (TMTSF: tetramethyltetraselenafulvalene) are generated at a (TMTSF)₂PF₆ single crystal–solution interface.⁶ Our initial experiment was aimed at the epitaxial electrodeposition of (TMTSF)₂ClO₄, by performing an electrocrystallization of (TMTSF)₂ClO₄ onto a (TMTSF)₂PF₆ isostructural template in dichloromethane at 40 °C. Due to the higher solubility of the materials at this temperature, the increased diffusion length of the oxidized species away from the electrode allowed a seeding of the electrocrystallization cell with (TMTSF)₂PF₆ single crystals and was assumed to yield (TMTSF)₂ClO₄ epitaxial overlayers on the seeding crystal. However, a control experiment showed that a simple immersion of a (TMTSF)₂PF₆ seed crystal in a dichloromethane solution containing ClO₄[−] anions at the same temperature results in the generation of (TMTSF)₂ClO₄ overlayers.⁶ Therefore, we could not conclude at that time that the thin film formations were exclusively due to an electrodeposition process. Subsequent studies of samples obtained through solely an immersion process, by scanning electron microscopy (SEM) with microanalysis via energy dispersive spectrometry (EDS), have shown that the superconducting overlayers obtained in dichloromethane at 40 °C are rather irregular and distributed over the various faces of the crystal template.⁷

Following experiments showed that these overlayer formations are highly solvent dependent. In the present report, we wish to give the most significant results obtained in 1,1,2-trichloroethane (TCE) for two kinds of different experiments: (i) (TMTSF)₂PF₆ template immersions in TCE solutions containing ClO₄[−] and TMTSF; (ii) an electrochemically mediated process, using exactly the same electrolyte solution, in an electrocrystallization cell operated at a very low (1.2 ×

(1) See for example: Tredgold, R. H. *Order in Thin Organic Films*; Cambridge University Press: New York, 1993. Ulman, A. *An Introduction to Ultrathin Organic Films: From Langmuir–Blodgett to Self-Assembly*; Academic Press: New York, 1991.

(2) Kawabata, K.; Tanaka, K.; Mizutani, M. *Adv. Mater.* **1991**, *3*, 157.

(3) Moldenhauer, J.; Wachtel, H.; Schweitzer, D.; Gompf, B.; Eisenmenger, W.; Bele, P.; Brunner, H.; Keller, H. J. *Synth. Met.* **1995**, *70*, 791.

(4) Niebling, U.; Steinl, J.; Schweitzer, D.; Strunz, W. *Solid State Commun.* **1998**, *106*, 505.

(5) (a) Hillier, A. C.; Maxson, J. B.; Ward, M. D. *Chem. Mater.* **1994**, *6*, 2222. (b) Last, J. A.; Hillier, A. C.; Hocks, D. E.; Maxson, J. B.; Ward, M. D. *Chem. Mater.* **1998**, *10*, 422 and references therein.

(6) Ribault, M.; Moradpour, A. *J. Am. Chem. Soc.* **1998**, *120*, 7993.

(7) Moradpour, A.; Ribault, M.; Auban-Senzier, P. *Adv. Mater.* **2000**, *12*, 719.

10^{-3} $\mu\text{A}/\text{mm}^2$) current density. As might be expected from the anisotropic properties of the template $(\text{TMTSF})_2\text{PF}_6$ single crystals, we find that the formation of the $(\text{TMTSF})_2\text{ClO}_4$ overlayers, obtained by the immersion of the template in TCE electrolyte solutions, is in fact *highly anisotropic* and leads to the formation of well-defined $(\text{TMTSF})_2\text{ClO}_4$ thin films *exclusively over specific crystal faces*. In addition, we identify unambiguously the electrochemically mediated epitaxial growth of $(\text{TMTSF})_2\text{ClO}_4$ overlayers for the first time. This is based on the interesting fact that the electrochemically generated overlayers are obtained on substrate crystal faces distinct from those involved in the immersion experiments. The conductivity of the $(\text{TMTSF})_2\text{ClO}_4$ film formed along a single crystallographic direction of the template by the immersion process is reported.

Experimental Section

TMTSF was synthesized⁸ and purified⁹ according to the literature, and $(\text{TMTSF})_2\text{PF}_6$ single crystals were prepared as previously described.⁶ In the immersion experiments, the template $(\text{TMTSF})_2\text{PF}_6$ crystals (typical sizes: $10 \times 1 \times 0.5$ mm) were introduced into an anhydrous TCE solution, containing TMTSF (3×10^{-3} M) and a large excess (0.1 M) of *n*-tetrabutylammonium perchlorate. The tightly closed vessels were maintained at room temperature with oxygen excluded. For the electrochemical film overgrowth, the template $(\text{TMTSF})_2\text{PF}_6$ crystal was placed into a standard electrocrystallization cell containing the same solution at room temperature and operating at a very low current density (1.2×10^{-3} $\mu\text{A}/\text{mm}^2$). In these electrocrystallization experiments, and in contrast to the immersion experiments, some additional TMTSF cation radicals are generated and partly diffuse toward the template single crystal because of the low current density. This process avoids the saturation concentration to be reached easily and consequently the nucleation of $(\text{TMTSF})_2\text{ClO}_4$ to occur exclusively on the electrode (this procedure is an alternative to increasing the cell temperature as used previously⁶). Subsequently to the immersion and electrochemical experiments, the crystals were harvested and one part of each was fixed with silver paste onto sample holders for electron microscopy.

Scanning electron microscopy (SEM) images were acquired at room temperature using a Philips XL30 microscope. The electron beam energy was 10 keV. Qualitative X-ray chemical analysis of the crystal surfaces was performed by means of an energy dispersive spectrometer (EDS) containing a germanium-diode X-ray detector (Princeton Gamma-Tech, Inc., Princeton, NJ). The recorded X-ray spectra involved fluorine, chlorine, phosphorus, and selenium as the analyzed elements, and the corresponding analyzed depth was estimated to be lower than $3 \mu\text{m}$. The thickness of the generated $(\text{TMTSF})_2\text{ClO}_4$ films was determined from EDS X-ray maps performed on sections of $(\text{TMTSF})_2\text{PF}_6$ crystals cut along their *bc* plane (see the crystal section in Figure 1).

The molecular organization of the $(\text{TMTSF})_2\text{PF}_6$ triclinic crystal structure¹⁰ was simulated by the CarIne Crystallography 3.1 program¹¹ using published unit-cell dimensions and atomic coordinates.¹² The view of the crystal cross section (Figure 1) resulted from simulated cuttings performed along

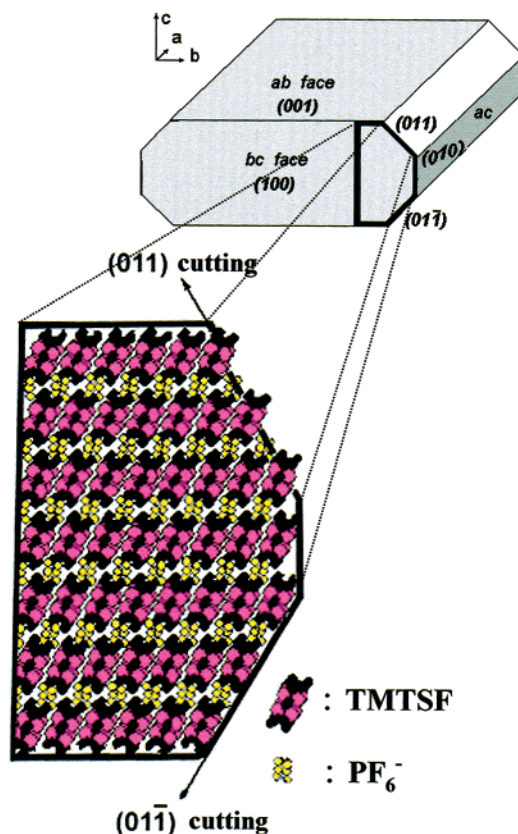


Figure 1. (i) Indexing of the crystal faces of the needlelike $(\text{TMTSF})_2\text{PF}_6$ single crystal. (The fastest crystal growth rate is along the *a* direction and results in the largest crystal surfaces corresponding to the (001) faces.) (ii) In color: The simulated molecular organization of the $(\text{TMTSF})_2\text{PF}_6$ crystal structure. (The molecular “roughness” of the (011) face is emphasized by the line symbolizing the (011) cutting corresponding to the (011) crystal plane that bisects the TMTSF units; compare to the flatness of the $(0\bar{1}\bar{1})$ cutting.)

the (001), (010), (011), and $(0\bar{1}\bar{1})$ crystallographic planes. This simulation allowed us to identify the chemical units (molecules or ions) constituting the actual crystal surfaces and consequently to determine the units exposed at the crystal/solution interfaces when $(\text{TMTSF})_2\text{PF}_6$ is brought into contact with an electrolyte.

To demonstrate the superconductivity of the generated $(\text{TMTSF})_2\text{ClO}_4$ film, four gold contacts were evaporated exclusively on the $(0\bar{1}\bar{1})$ face of the sample. The resistances were measured with low-frequency current injection and lock-in detection. Conductivity measurements were then performed down to 0.5 K in a ^3He refrigerator. The thickness (usually within $5\text{--}15 \mu\text{m}$ from one sample to another) of the investigated $(\text{TMTSF})_2\text{ClO}_4$ film was $10 \mu\text{m}$. The sample was slowly cooled to around the ordering transition of the ClO_4 anion (24 K) in order to obtain the relaxed state.¹³

Results

First, it is worth recalling the indexing of the various crystallographic faces of a $(\text{TMTSF})_2\text{PF}_6$ single-crystal template with an emphasis on the corresponding schematic molecular organization of the crystal (Figure 1).¹⁴ Taking into account the highly anisotropic nature of the template crystals we have investigated the possibility to generate $(\text{TMTSF})_2\text{ClO}_4$ overlayers at the interfaces of every distinct crystal surfaces with the electrolyte,

(8) Moradpour, A.; Peyrussan, V.; Bechgaard, K. *J. Org. Chem.* **1983**, *48*, 388.

(9) Moradpour, A.; Bechgaard, K.; Barrie, M.; Lenoir, C.; Murata, K.; Laco, T. C.; Ribault, M.; Jerome, D. *Mol. Cryst. Liq. Cryst.* **1985**, *119*, 69.

(10) Bechgaard, K. *Mol. Cryst. Liq. Cryst.* **1982**, *79*, 1 and references therein.

(11) Boudias, C.; Monceau, D. CarIne Crystallography 3.1, Senlis, France, 1989.

(12) Gallois, B.; Gaultier, J.; Hauw, C.; Lamcharfi, T.; Filhol, A. *Acta Crystallogr.* **1986**, *B42*, 564.

(13) Ishiguro, T.; Yamaji, K. *Organic Superconductors*; Springer-Verlag: Berlin, 1990.

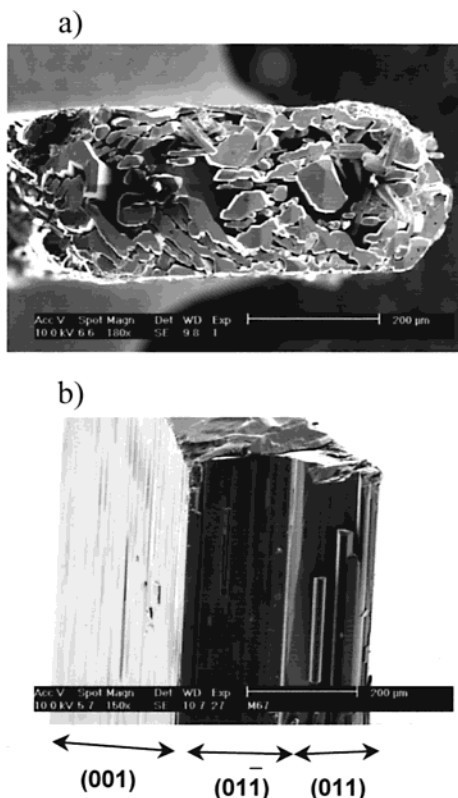


Figure 2. SEM images of a $(\text{TMTSF})_2\text{PF}_6$ single crystal immersed for 6 days at 22 °C in TCE solution (see Experimental Section): (a) view of the top bc section plane of the crystal showing crystallites grown along the a direction; (b) side view of the adjacent crystal faces (001), (011), and (011). The (010) face of this crystal is not visible because of its extremely narrow width;¹⁴ the top part of the crystal, where the crystallites growth occurs, was removed by cutting the crystal along bc plane before this image was recorded.

considering the two different (immersion and electrochemical) experimental procedures.

(i) $(\text{TMTSF})_2\text{ClO}_4$ Film Formation by the Immersion Procedure. The $(\text{TMTSF})_2\text{PF}_6$ single crystal was immersed for 6 days in TCE electrolyte solution at room temperature. The immersion process results in both *morphological* and *chemical* modifications of the various crystal faces. The development of $(\text{TMTSF})_2\text{ClO}_4$ overlayers was established, identifying the surface regions containing chlorine, by EDS analysis. The SEM and EDS analysis images reveal the following significant modifications of the faces (Figure 2): (i) Nucleation and nonuniform growth of crystallites in the a direction are observed on the bc section (Figure 2a); the composition of these crystallites corresponds to $(\text{TMTSF})_2\text{ClO}_4$ as determined by EDS analysis. (ii) A slight surface dissolution of the (001) face takes place as indicated by the increased roughness (Figure 2b) as compared to the starting crystal; however *no chemical modification* is detected on this surface by EDS analysis (not shown). (iii) By contrast, the morphologically undamaged neigh-

(14) The electrochemically grown $(\text{TMTSF})_2\text{PF}_6$ single crystals usually exhibit either six or eight lateral faces corresponding to respectively hexagonal or octagonal sections (only the latter is schematized in Figure 1). A hexagonal section results from the vanishing of the (010) faces; the present sample involves undetectably small (010) faces (see the right side of Figure 2a), and consequently the shape of the presently investigated section is hexagonal type exhibiting only the (011) and (011) lateral faces.

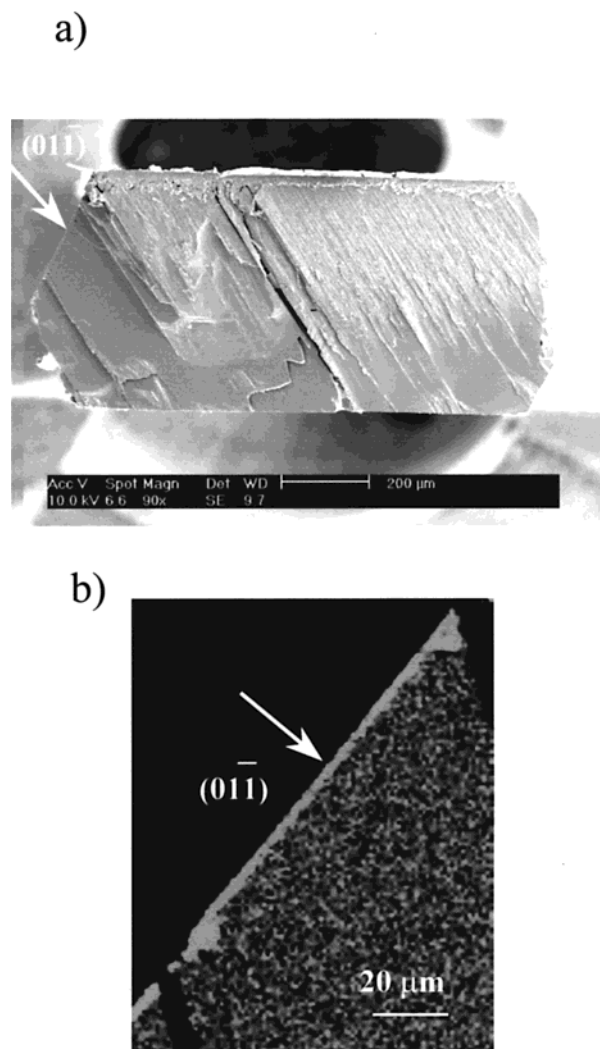


Figure 3. (a) SEM image of the $(\text{TMTSF})_2\text{PF}_6$ crystal section, after immersing in TCE solution for 6 days at 22 °C; the top part of the crystal was removed before recording this image. (b) EDS microanalysis emphasizing the chlorine (ClO_4) containing areas (grey); the darker portion represents the chlorine-free $(\text{TMTSF})_2\text{PF}_6$ substrate. The magnification for recording the X-ray map was 750.

boring (011) faces (Figure 2b) exhibit the formation of a *continuous $(\text{TMTSF})_2\text{ClO}_4$ overlayer* on the whole crystal surface as detected by EDS analysis (not shown). (iv) The (010) face is not visible,¹⁴ and on the next (011) face, the growth of several crystallites of significant size ($(\text{TMTSF})_2\text{ClO}_4$ material as deduced from EDS analysis) is observed (Figure 2b). These crystallite formations have never been observed on the previous (011) faces in any case.

After removal of the top part of the crystal by cutting it along the bc plane, the exposed cross section was investigated by SEM (Figure 3a). The cross-sectional EDS analysis (Figure 3b) clearly indicates the formation of a well-defined $(\text{TMTSF})_2\text{ClO}_4$ film on the (011) face with a thickness of nearly 5 μm.¹⁵

The temperature dependence of the zero-field resistance of the $(\text{TMTSF})_2\text{ClO}_4$ film below 16 K is shown in Figure 4. The curve clearly exhibits the metal to spin

(15) The dependence of the film thickness on the salt concentration and the temperature, as well as on the surface area of the crystal, will be reported in a forthcoming paper.

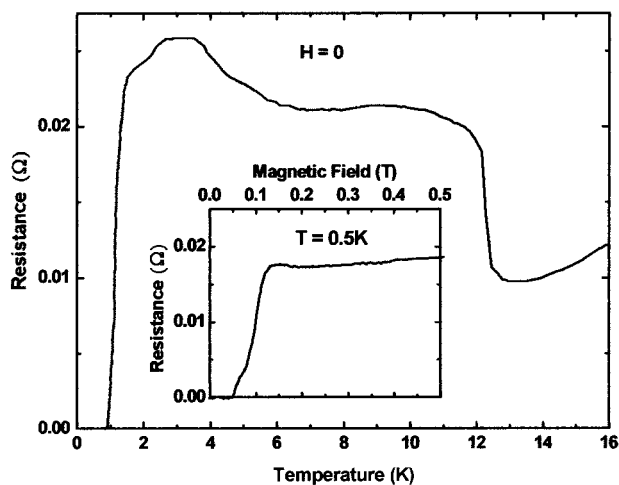


Figure 4. Temperature dependence of the zero-field $(\text{TMTSF})_2\text{ClO}_4$ film resistance (insert: low-field magnetoresistance of the film at $T = 0.5$ K).

density wave (SDW) transition at 12 K specific to the $(\text{TMTSF})_2\text{PF}_6$ template.¹³ As the temperature is further decreased, the resistivity initially increases due to a lower penetration of the current lines into the substrate related to its increasing insulating SDW behavior. For temperatures below 3.5 K, the film exhibits the properties of $(\text{TMTSF})_2\text{ClO}_4$ alone since its resistivity decreases toward a sharp superconducting transition with an onset critical temperature of $T_c \approx 1.4$ K. Superconductivity is suppressed (Figure 4, insert) by a low magnetic field of about 0.15 T, similar to the critical field of the bulk $(\text{TMTSF})_2\text{ClO}_4$ crystals.¹³ The extrapolated zero-temperature normal-state resistance yields a film resistivity of $\rho = 10 \mu\Omega\cdot\text{cm}$, a value comparable to bulk samples; however, the contact geometry prevented us from calculating the actual ρ_a film resistivity at any given temperature.

(ii) Electrochemically Mediated $(\text{TMTSF})_2\text{ClO}_4$ Film Formation. The $(\text{TMTSF})_2\text{PF}_6$ single-crystal template was maintained in a same TCE solution containing TMTSF and the ClO_4^- electrolyte in an electrocrystallization cell, working at a very low current density at room temperature, for the same duration as the immersion procedure (6 days). The subsequent SEM and EDS analysis (Figure 5) showed several surface modifications already observed above (because of the immersion in the electrolyte) but also an interesting new event related to the electrochemical process that was not detected in the previous immersion experiment: (i) The formation of the same kind of $(\text{TMTSF})_2\text{ClO}_4$ crystallites on the bc section of the crystal (not shown) was seen, as previously observed in Figure 2a. (ii) A continuous $(\text{TMTSF})_2\text{ClO}_4$ thin film on the $(01\bar{1})$ faces is still observed (see EDS analysis of this face in Figure 5b). (iii) On the (011) faces $(\text{TMTSF})_2\text{ClO}_4$ crystallites are again detected (not shown). (iv) On the (001) faces (previously unchanged) new modifications are now detected by EDS analysis (Figure 5); $(\text{TMTSF})_2\text{ClO}_4$ island overlayers are formed on these crystal surfaces. The thickness of the islands is estimated to be at least $3 \mu\text{m}$ because the underlying $(\text{TMTSF})_2\text{PF}_6$ template was not detected by EDS. However, because of the discontinuous shape of the $(\text{TMTSF})_2\text{ClO}_4$ overgrown layers, no transport measurements could be performed

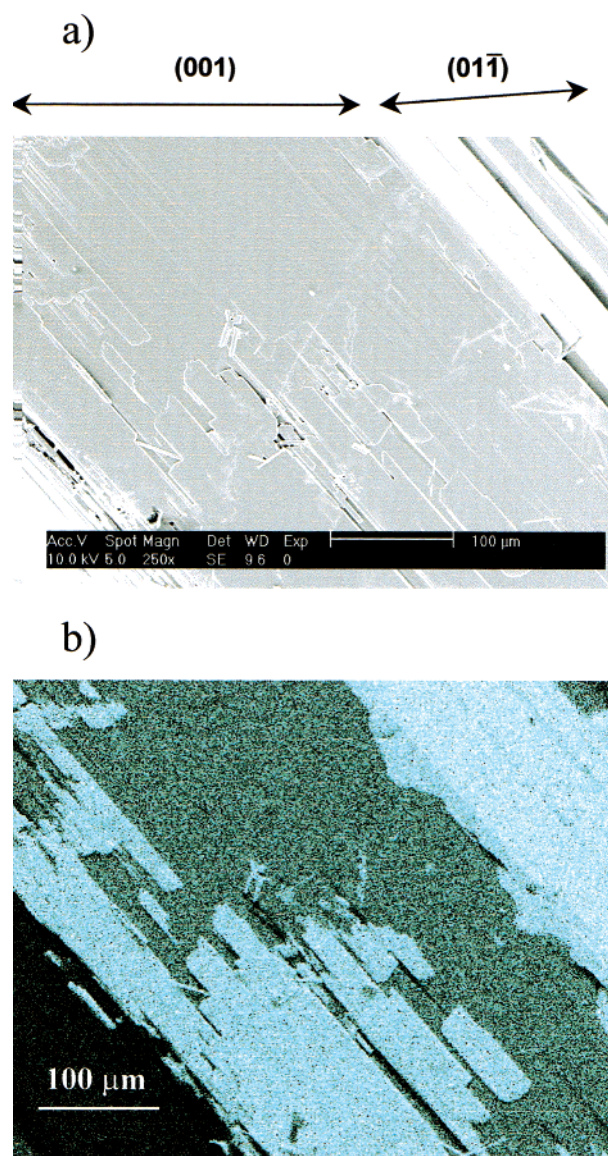


Figure 5. Images of an electrochemically mediated epitaxy at 22°C in TCE solution onto a $(\text{TMTSF})_2\text{PF}_6$ single-crystal template: (a) SEM image of the (001) and $(01\bar{1})$ faces; (b) EDS microanalysis identifying the chlorine (ClO_4) containing island overlayers (bright blue) grown on the largest (001) face of the sample. Note the simultaneous formation of the $(\text{TMTSF})_2\text{ClO}_4$ film (bright blue) on the neighboring $(01\bar{1})$ face formed by ion exchange. The magnification for recording the EDS image was 250.

on this modified (001) face, though the formation of a $(\text{TMTSF})_2\text{ClO}_4$ film by an electrochemically mediated epitaxy is established for the first time. Full coverage of this face should be obtained by longer periods of electrochemically mediated epitaxy.

Discussion

The different kinds of face selective modifications¹⁶ observed in the present study are classified for convenience in two types: (i) Surface morphological and/or chemical "rearrangements" of the starting $(\text{TMTSF})_2\text{PF}_6$ single-crystal template with no external supply of TMTSF cation radicals are seen; these modifications

(16) Hillier, A. C.; Ward, M. D. *Science* **1994**, *263*, 1261.

either involve $(\text{TMTSF})_2\text{ClO}_4$ crystallite formations related to a clear dissolution/recrystallization process or a continuous $(\text{TMTSF})_2\text{ClO}_4$ film formation without overgrowth (*vide infra*) on the entire morphologically preserved crystal faces. (ii) Electrochemically mediated $(\text{TMTSF})_2\text{ClO}_4$ overlayer formations are observed; the overgrowth process in this case is designated as "epitaxial" because it is related to an additional electrochemical supply of TMTSF cation radicals (although the crystallite formations obtained by the dissolution/recrystallization of the starting crystals could also be considered to involve epitaxy).

To account for the highly anisotropic behavior of the different faces of the template in the present immersion and electrochemical experiments, let us consider the surface molecular organization of the $(\text{TMTSF})_2\text{PF}_6$ crystal (Figure 1). The structure of the investigated one-dimensional conductor involves stacks of TMTSF molecules along the *a* direction forming sheets along the *b* axis, which alternate with sheets built by PF_6 anions. Therefore, the (001) face is either terminated by TMTSF molecules (as depicted in Figure 1) or by PF_6 anions. However, no "communication" of further sheets beneath these surface layers with the surrounding electrolyte is possible. On the other hand, for both (011) and $(0\bar{1}\bar{1})$ faces, channels of anions which communicate with the electrolyte are easily identified. However, it is worth emphasizing the distinct "molecular asperity" of the faces obtained along the (011) cuts including portions of TMTSF molecules that protrude from an average surface plane, as compared to the molecularly flat $(0\bar{1}\bar{1})$ face (Figure 1).

On the basis of the above simple picture, a rational account of these highly anisotropic crystal surface modifications could be considered. The $(\text{TMTSF})_2\text{ClO}_4$ crystallite growth involves partial dissolution of the $(\text{TMTSF})_2\text{PF}_6$ template and subsequent recrystallization of $(\text{TMTSF})_2\text{ClO}_4$ as microcrystals because of the large concentration excess of ClO_4 compared to PF_6 anions. This crystallite growth occurs on the (100) *bc* sections and on the (011) faces according to the fastest growth rate direction along the *a* axis. Whereas the crystallite formations on the *bc* sections along this favored growth direction is not surprising, it is remarkable that all faces of the template other than the (011) ones are free from

such crystallite formations (Figure 2). Thus the actual surface topology of the (011) faces, simulated as molecularly rough, implies a larger number of nucleation sites that presumably come from a surface reconstruction. However the true structure of these surfaces is presently not yet known. In addition to the elegant AFM¹⁷ and STM¹⁸ studies, devoted exclusively to the largest (001) faces of such TMTSF cation-radicals salts, supplementary structural studies are therefore needed here.

The generation of the $(\text{TMTSF})_2\text{ClO}_4$ film on the morphologically preserved $(0\bar{1}\bar{1})$ face excludes surface dissolution phenomena and does not appear to involve any deposition of solute species. In fact in a separate experiment¹⁹ we find that the masking of half of a $(0\bar{1}\bar{1})$ face by gold evaporation results in the generation of a $(\text{TMTSF})_2\text{ClO}_4$ layer originating from the outermost surface (gold level) and proceeding to the bulk of the crystal template. This implies ingress of perchlorate anions rather than an overgrowth process. Therefore this film generation is presumably due to an uncommon kind of an ion-exchange process.²⁰ Whether this ion exchange involves the existing anions' channels opened to the electrolyte solution (Figure 1) or is related to other pathways needs further studies.

On the other hand, the growth of the electrochemically generated epitaxial island films, implying an additional electrochemical supply of TMTSF cation radicals, takes place onto the largest (001) crystal faces free from anions' channels. This electrochemical epitaxial overgrowth involves the two fastest growth-rate directions (*a* and *b* axes) and takes place on a surface that is not chemically modified in the immersion experiments.

In summary, the $(\text{TMTSF})_2\text{ClO}_4$ thin film formation onto a $(\text{TMTSF})_2\text{PF}_6$ single crystal is strongly anisotropic and reflects the typical anisotropy of the template. The location of the generated well-defined films along specific crystallographic directions of the substrate and therefore their structural organization is controlled by the formation procedure based either on immersion or on electrochemically mediated epitaxy. The specific film parameters, such as thickness and/or integrity, are controlled by adjustment of the immersion or electrochemical time periods. These results open the way to the elaboration of single-crystal superconducting thin films built onto distinct template crystal planes and to forthcoming possibly new physical properties.

CM000182W

(17) Carter, P. W.; Hillier, A. C.; Ward, M. D. *J. Am. Chem. Soc.* **1994**, *116*, 944.

(18) Li, S.; White, H. S.; Ward, M. D. *J. Phys. Chem.* **1992**, *96*, 9014.

(19) Angelova, A.; Auban-Senzier, P.; Moradpour, A. Unpublished results.

(20) To our knowledge, no ion-exchange property has been assigned as yet to these closely packed organic salts.